X-ray measurements of the strain and shape of dielectric/metallic wrap-gated InAs nanowires

J. Eymery, V. Favre-Nicolin, L. Fröberg, and L. Samuelson

Citation: Appl. Phys. Lett. **94**, 131911 (2009); doi: 10.1063/1.3114369
View online: http://dx.doi.org/10.1063/1.3114369
View Table of Contents: http://apl.aip.org/resource/1/APPLAB/v94/i13
Published by the American Institute of Physics.

X-ray measurements of the strain and shape of dielectric/metallic wrap-gated InAs nanowires

J. Eymery,[1,a)] V. Favre-Nicolin,[1] L. Fröberg,[2] and L. Samuelson[2]
[1]*CEA, INAC, SP2M, 17 rue des Martyrs, 38054 Grenoble Cedex 9, France*
[2]*Solid State Physics, Lund University, Box 118, S-221 00 Lund, Sweden*

(Received 10 December 2008; accepted 12 March 2009; published online 1 April 2009)

Wrap-gate (111) InAs nanowires (NWs) were studied after HfO_2 dielectric coating and Cr metallic deposition by a combination of grazing incidence x-ray techniques. In-plane and out-of-plane x-ray diffraction (crystal truncation rod analysis) allow determining the strain tensor. The longitudinal contraction, increasing with HfO_2 and Cr deposition, is significantly larger than the radial dilatation. For the Cr coating, the contraction along the growth axis is quite large (-0.95%), and the longitudinal/radial deformation ratio is >10, which may play a role on the NW transport properties. Small angle x-ray scattering shows a smoothening of the initial hexagonal bare InAs NW shape and gives the respective core/shell thicknesses, which are compared to flat surface values. © *2009 American Institute of Physics*. [DOI: 10.1063/1.3114369]

The horizontal and vertical nanowire (NW) integration into electronic and optoelectronic devices may require shell depositions to obtain for example refractive index adaptation for light guiding, electron/holes confinement, or dielectric/metallic wrap gate for transistors.[1] With the very small dimensions used in the recent devices, these coatings can strongly impact the NW active region, which must be carefully controlled during the integration process. Several important structural features have to be measured[2,3] such as the strain state and defect density that change the transport properties, or the shape and thickness inhomogeneity, which increase the leakage current or the electrostatic control. This letter will be focused on InAs NWs, which are used in resonant devices and transistors[4] for which very good characteristics have been observed in the vertical wrap-gated geometry.[5] The NW strain will be analyzed by grazing incidence x-ray diffraction (GIXRD) before and after HfO_2-dielectric and Cr-gate depositions, the measurements of crystal truncation rods (CTRs) giving access to longitudinal deformations and standard GIXRD to in-plane deformations. Grazing incidence small angle x-ray scattering (GISAXS) experiments will record the evolution of the NW initial hexagonal shape after the thin oxide and metallic depositions. It will allow extracting both the thickness of the core/shell structures and the surface shape smoothening.

The NW growth is gold assisted and takes place in a chemical beam epitaxy (CBE) system using trimethylindium, precracked *tertiary*-butylarsine, and precracked *tertiary*-butylphosphine as growth precursors. Prior to growth, size-selected Au aerosol particles are deposited on an $InAs(111)_B$ substrate and the sample is deoxidized in the growth chamber at 520 °C under As pressure. The NW density is selected to be about 0.55 ± 0.02 NW/μm^2. HfO_2-dielectric has been deposited on the InAs NW samples by atomic layer deposition at 100 and 250 °C during the same time to check the influence of process temperature. Finally, the Cr gate has been deposited at room temperature by sputtering.[6,7] As shown in Fig. 1, the NW growth is well oriented and the narrow orientation distribution allows studying the NW using their epitaxial relation with the substrate lattice.[2] We use the (hkl) Miller indices corresponding to the $InAs(111)_B$ surface unit cell with hexagonal surface unit cell vectors $a_1 = 1/2[\bar{1}10]$, $a_2 = 1/2[0\bar{1}1]$, and $a_3 = [111]$. Within this basis, $InAs(111)_B$ bulk Bragg reflections are found at $l = 1,4,7\ldots$ for $(h,k) = (1,0)$ and at $l = 2,5,8\ldots$ for $(h,k) = (0,1)$. Microscopy experiments have shown a hexagonal shape for the bare NWs.[8] X-ray experiments were performed at the European Synchrotron Radiation Facility (ESRF, Grenoble France) under helium flow to prevent sample degradation and air diffuse scattering. Data were collected on the BM32 and D2AM French CRG beamlines with photon energy of 9.561 keV

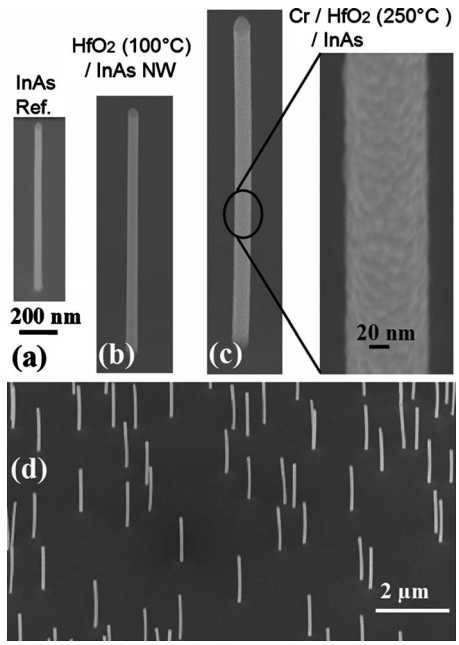

FIG. 1. SEM images of reference (a) and core/shell [(b) and (c)] (111) InAs NWs grown by CBE. (b) corresponds to HfO_2-shell grown at 100 °C on a reference sample similar to (a) and (c) to a Cr-shell grown on HfO_2/InAs (oxide growth is performed at 250 °C). (d) shows a tilted view of the later NW assembly. Note that the tilt angles of the images are different and that the diameters can be deduced from the scale bars.

a)Electronic mail: joel.eymery@cea.fr. Present address: Équipe mixte CEA-CNRS, Nanophysique et Semiconducteurs.

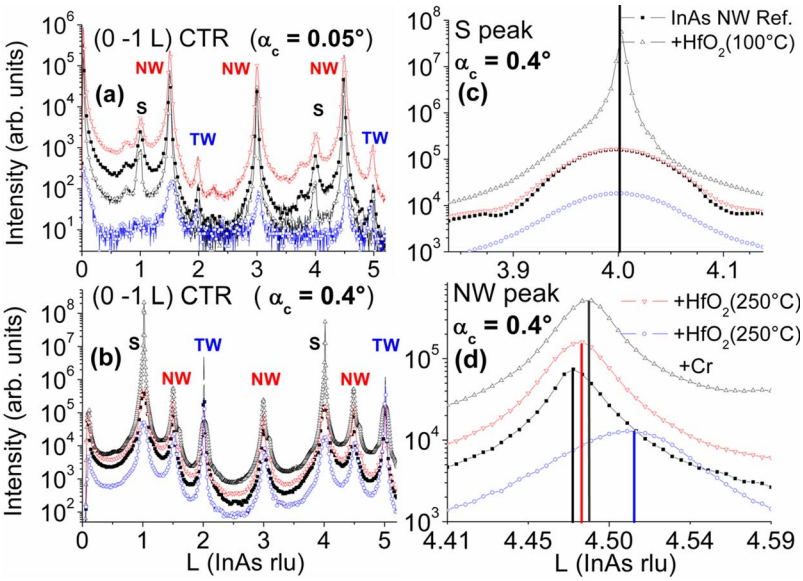

FIG. 2. (Color online) $(0\bar{1}l)$ CTR measurements of the reference and core/shell NWs shown in Fig. 1 for two grazing incidences (a) α=0.05° and (b) 0.4°. l is in reciprocal lattice units of the cubic InAs (111) substrate (marked by *S*). Magnifications of the ZB substrate peaks at l=4 (c) and of the wurtzite NW peaks at l =4.5 (d). TW corresponds to twinned ZB substrate overgrowth.

giving very close critical angles of total reflection for InAs and Cr (respectively, 0.305° and 0.316°).

$\langle h00\rangle$, $\langle 0h0\rangle$, and $\langle hh0\rangle$ (h=1,2,3) in-plane reflections have been first measured at α=0.2° for the four samples: InAs reference, HfO_2-deposited (at 100 and 250 °C) and Cr deposited on the HfO_2-250 °C NW. No significant shifts of the Bragg peak positions can be measured except for the Cr-coated sample giving +0.06% ± 0.03% dilatation.[7] Radial scan widths (sensitive to strain) are almost constant for bare and HfO_2(250 °C)-coated NWs, whereas we observed a broadening proportional to the diffraction order, small for HfO_2(100 °C) and larger for Cr deposition.[7] This indicates an increase of the radial strain distribution in the NW assembly, especially after Cr coating.

Figure 2 shows the $(0\bar{1}l)$ CTR measurements for the four samples and two grazing incidence angles (α=0.05° and 0.4°) below and above the critical angles of total reflection, respectively. Changing the incidence angle allows to separate the NW from the substrate and overgrowth contributions.[2] The indexation is also in agreement with complementary $(0\bar{2}l)$ CTRs measurements for the same grazing angles, and with CTRs measurements at intermediate angle (α=0.2°) where the multiple beam scattering effects (i.e., peak splitting) are clearly observed for the NWs. Zinc blende (ZB) peaks at l=1,4 refer to substrate (*S*). They are very weak at small grazing incidence and more intense at larger angle. Twinned ZB peaks at l=2,5 (noted TW) correspond to substrate overgrowth and follow the same behavior as a function of α. The NW scattering is measured at l=1.5, 3, and 4.5 and corresponds to the [111] wurtzite growth direction. Its intensity does not decrease with α and is still clearly observed in the transmission regime [α=0.5°, Fig. 2(a)]. This behavior applies both to the reference and to the core/shell samples, the most striking feature being the CTR broadening for the Cr deposited sample (already observed for in-plane diffraction). As shown in Fig. 2(c) (for α=0.4° and l=4), the positions of the substrate peaks are nearly insensitive to α and to the dielectric and metallic deposition. It gives an internal reference of the lattice distance/deformation and allows checking the experimental accuracy. The error bar on the *S*-peak position measurements is estimated to ±0.065% considering the measurements at three grazing incidences (0.05°, 0.2°, and 0.4°), two CTRs [$(0\bar{1}l)$, $(0\bar{2}l)$], and four l-values (1, 2, 4, and 5). The NW deformation along the growth direction is measured directly from the $\Delta l/l$ variation between the reference and the core/shell structures. As shown in Fig. 2(c) corresponding to α=0.4° and l=4.5, the NW peaks exhibit small shifts for HfO_2-coated NWs and larger for Cr-coated one. The contractions of the core/shell NWs along the growth direction are −0.95% ± 0.07% for Cr/HfO_2 (T=250 °C)/InAs and −0.13 (respectively, −0.26) ±0.07% for HfO_2/InAs grown at 250 °C (respectively, 100 °C). These strains are larger compared to the low in-plane values, which are significant only for the Cr-deposited sample (+0.06% ± 0.03%). Although the mechanical boundary conditions are different, the large experimental NW Poisson's ratio ρ between the longitudinal and the radial strain may be compared to the strain distribution calculated for cylindrical misfit-strained core-shell NWs with continuum calculation and isotropic elasticity constants. The analytical solution of this core/shell elasticity problem[9] gives a constant ratio $\rho=2(1-\nu)/(1-3\nu)$, where ν is the isotropic Poisson's ratio of the core/shell materials (supposed equal). This ratio does not depend on lattice mismatch and surface stress and for ν=0.27,[10] we get $\rho\approx 7.7$, which may confirm the large experimental value of the longitudinal strain with regard to the radial one (>10).

The average NW shape and size is measured by using small-angle scattering at grazing incidence and emergence ($\alpha=\beta$=0.27°). Figure 3 shows intensity measurements I(ψ) as a function of the in-plane scattering angle (ψ) for several sample orientations defined by the azimuth ξ around the surface normal. For the InAs NW reference [see Fig. 3(a)], the systematic measurement of I(ψ) as a function of ξ exhibits a 30° symmetry in agreement with the hexagonal shape.[2] The origin ξ=0° is defined by a direction perpendicular to the NW facets [see the inset in Fig. 3(c)]. The main features of the bare InAs NWs azimuth-angle dependence consist of the damping and the shift of the second-order fringe from ξ =0° to 30° and of the strong decrease in intensity of the third oscillation at ξ=30°.[2] The facet width R of a regular hexagon calculated from a distorted wave born approximation

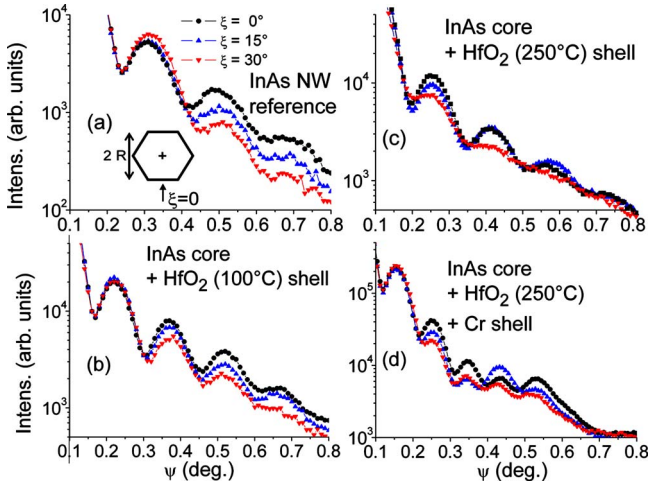

FIG. 3. (Color online) GISAXS profiles of the NW samples shown in Fig. 1 for several incoming beam directions ξ [see the inset of (a)] with respect to the NW hexagonal shape. (a) is the uncoated InAs NW, (b) [respectively, (c)] HfO_2-shell grown on sample similar to reference (a) at 100 °C (respectively, 250 °C), and (d) Cr-shell grown on NW similar to (c). ψ corresponds to the in-plane scattering angle, incidence and emergence are 0.27° and the wavelength is 0.12968 nm.

(DWBA) analysis[11] is 18.2 ± 0.5 nm with a Gaussian size distribution lower than 7%.[2] The dielectric deposition alters these features indicating a change in shape, probably induced by the very different growth mechanisms.[7] The modification depends on the HfO_2 deposition temperature [see Figs. 3(b) and 3(c)] and a complete analysis of GISAXS bidimensional mappings including the core/shell scattering geometry should bring more quantitative information. The Cr deposition gives higher frequency fringes [Fig. 3(d)] corresponding to a thicker shell. The core/shell thicknesses have been analyzed in a very simple way comparing the positions of the first four intensity minima for $\xi=0$ to the DWBA calculations for a *hexagonal shape*. For HfO_2-coated NWs grown at 250 °C (respectively, 100 °C) and Cr/HfO_2-coated NWs, we get, for the total facet width R, 21.9 (24.2) and 37.0 nm, respectively. By difference with the initial bare NW value (18.2 nm), we get 3.7 (6.0) nm for the HfO_2 thicknesses and 15.1 nm for the Cr thickness. An error bar (± 0.5 nm) may be estimated from the DWBA calculations with the cylindrical shape.[12] These values can be compared to the planar growth in between the NWs, which can be estimated by x-ray reflectivity.[7] Indeed, the specular reflection remains large enough due to the very low NW density, and the oscillation fringe spacings gives 4.9 (7.5) nm for HfO_2 and 45 nm for the Cr thicknesses. This comparison shows that the HfO_2 growth on the NW side is roughly equivalent to the flat surface one, but that the Cr deposition is lower by a factor of 3. It also confirms that the low temperature HfO_2 deposition leads to thicker layer/shell.[7]

In conclusion, hexagonal (111) InAs NWs ($R \approx 18.5$ nm) have been studied at different steps of transistor wrap-gate integration. A combination of grazing incidence x-ray techniques has been used to get core/shell geometries (shape and thickness) and internal elastic relaxations. The strain tensor exhibits a very large anisotropy due to surface relaxation and (111) growth orientation. 4 (6) nm HfO_2 deposition at 250 °C (100 °C) induces a longitudinal contraction strongly enlarged by a 15 nm Cr shell (−0.95%) and the radial expansion is very small. This deformation should strongly affect the electron mass in transistor devices as well as the optical properties of NW-based core/shell heterostructures.[7,13]

This work has been performed under the EU-program NODE Grant No. 015783. The authors would like to thank the French CRG ESRF beamlines for their technical helps.

[1] C. Thelander, P. Agarwal, S. Brongersma, J. Eymery, L. F. Feiner, A. Forchel, M. Scheffler, W. Riess, B. J. Ohlsson, U. Gösele, and L. Samuelson, Mater. Today **9**, 28 (2006).
[2] J. Eymery, F. Rieutord, V. Favre-Nicolin, O. Robach, Y. M. Niquet, L. Fröberg, T. Mårtensson, and L. Samuelson, Nano Lett. **7**, 2596 (2007).
[3] S. O. Mariager, C. B. Sørensen, M. Aagesen, J. Nygård R. Feidenhans'l, and P. R. Willmott, Appl. Phys. Lett. **91**, 083106 (2007).
[4] T. Bryllert, L.-E. Wernersson, T. Löwgren, and L. Samuelson, Nanotechnology **17**, s227 (2006).
[5] C. Thelander, L. Fröberg, C. Rehnstedt, L. Samuelson, and L.E. Wernersson, IEEE Electron Device Lett. **29**, 206 (2008).
[6] L. E. Fröberg, C. Rehnstedt, C. Thelander, E. Lind, L.-E. Wernersson, and L. Samuelson, IEEE Electron Device Lett. **29**, 981 (2008).
[7] See EPAPS Document No. E-APPLAB-94-016914 for growth details, in-plane GIXRD and reflectivity measurements, and comments on the influence of shape on electrical measurements. For more information on EPAPS, see http://www.aip.org/pubservs/epaps.html.
[8] M. W. Larsson, J. B. Wagner, M. Wallin, P. Håkansson, L. E. Fröberg, L. Samuelson, and L. R. Wallenberg, Nanotechnology **18**, 015504 (2007).
[9] V. Schmidt, P. C. McIntyre, and U. Gösele, Phys. Rev. B **77**, 235302 (2008).
[10] S. W. Ellaway and D. A. Faux, J. Appl. Phys. **92**, 3027 (2002); We use for consistency with the model of Ref. 9 the isotropic Poisson ratio $\nu_{iso} = c_{12}/[2(c_{12}+c_{44})] \approx 0.27$. Semi-empirical calculations, confirming also the large ratio between the longitudinal and radial strain, prefers usually the Poisson's ratio along the NW growth $\nu_{111} = 2(c_{11}+2c_{12}-2c_{44})/(c_{11}+2c_{12}+4c_{44}) \approx 0.57$.
[11] R. Lazzari, J. Appl. Crystallogr. **35**, 406 (2002).
[12] The minima of the oscillation fringes for HfO_2 and Cr deposited samples have been also fitted with a cylindrical model. The radius value R is 4.9 (8) nm for the HfO_2 grown at 250 °C (100 °C) and 16.1 nm for the Cr deposition. These results are close to the values obtained with the hexagonal shape, and allow estimating an error bar of about ±0.5 nm for the shell thicknesses.
[13] Y. Hori, Y. Ando, Y. Miyamoto, and O. Sugino, Solid-State Electron. **43**, 1813 (1999).